New TiO$_2$ Double Layer Nano Particulate Photo Anode for Highly Efficient Dye Sensitized Solar Cells (DSSC)

Goran Kilibarda[1,2] , Sabine Schlabach[1], Dorothée Vinga Szabó[1], Thomas Hanemann[1,2,]*

[1]Karlsruher Institut für Technologie (KIT), Institut für Angewandte Materialien, Hermann-von-Helmholtz-Platz 1, 76344 Eggenstein-Leopoldshafen, Germany
[2]Universität Freiburg, Institut für Mikrosystemtechnik, Georges-Köhler-Allee 102, 79110 Freiburg, Germany
[*]E-mail: thomas.hanemann@kit.edu

In this work, a new process chain for the realization of high performance dye sensitized solar cells (DSSC) will be introduced. The photo anode consists of two titania layers, the first layer facing the FTO/glass substrate is fabricated by spin coating using a commercial titania (P25), the second one is deposited by gas phase synthesis. Different synthesis parameters, optional post treatments, two different sensitizers and three different electrolyte mixtures have been systematically varied to optimize the photovoltaic conversion properties. A good efficiency value around 9.1% could be realized after comprehensive process evaluation.

1. INTRODUCTION

In addition to the established inorganic semiconductor based photovoltaic cells [1-3] organic photovoltaic devices, especially the dye sensitized solar cell (DSSC), have the potential to a future commercial success due to the low component and fabrication process costs as well as the capability of enabling flexible solar cells even for mobile applications. The DSSC was firstly presented by O'Regan and Grätzel 1991 as a new type of photoelectrochemical converter [4] and experienced a tremendous progress within a couple of years achieving an overall power conversion efficiency around 11% [5,6]. Since the beginning of this century this best research-cell efficiency remains more or less constant between 11 and 12 %, same is valid for other organic cell types [7]. The typical setup of a DSSC covers a working electrode (photo anode), mainly a mesoporous layer made of nano sized titania

(TiO_2) particles, deposited on a transparent conductive oxide electrode at the surface of a glass slide. At the surface of the titania layer (thickness 1-20 µm) a charge transfer dye, typically a ruthenium complex, which is responsible for the absorption of light and injection of an electron in the conduction band of the titania, is deposited. The circuit is continuously closed by a iodide/triiodide redox-shuttle, which is solved in a highly ionic conductive low viscous liquid electrolyte and platinum counter electrode [5,6]. Thus, low cost renewable energy harvesting can be performed with stable conversion rates even at elevated temperatures after 1000 hours [8]. In most of the cases the anatase phase of titania is used. In literature one can also find studies, where the good DSSC photovoltaic properties can be attributed to the cooperative effect of anatase and rutile phases together, due to facilitating charge separation and reduction of charge recombination [9-11]. A high DSSC efficiency can also be achieved by improving the light scattering properties of the anode material. The improvement of such light harvesting can be achieved by introduction of TiO_2 rough spheres as scattering centers [12-14]. To enhance the photovoltaic performances, additional post treatments of the TiO_2 photo anodes can be carried out, e.g. by the immersion of the titania layer in $TiCl_4$ solutions forming a thin TiO_2 blocking layer on the photo anode surface to suppress charge recombination and facilitate charge transport [15-17]. Additionally, oxygen plasma post treatments of photo anodes [15,18,19], increasing the surface hydrophilicity of TiO_2, enables an increased dye adsorption and hence a better improved photovoltaic performance. Recent developments are described in [20] and covers the surface modification of titania, the chemical variation of the sensitizer, the new emerging field of halide perovskites, the development of alternative electrolytes and redox shuttles and new counter electrodes. One key issue is still the nano structuring of the titania photo anode investigating e.g nano sheets [21] or nanotubes [22] allowing conversion efficiencies around 8.1 [21] or 9 % respectively [22].

The aim of this work is to demonstrate the performance of a double layer titania photo anode where the first layer is spin coated consisting of larger commercially available nano sized titania and a second layer, synthesized with the Karlsruhe Microwave Plasma Process (KMPP) of smaller nano sized particles [23]. It is expected, that the combination of particle sizes improves the photovoltaic performance by exploiting the advantages of each particle size. To investigate the influence of dye and electrolyte, systematic variation of different dyes and electrolytes were carried out. Additionally, post treatments with immersing photo anodes in a $TiCl_4$ solution and also exposure to oxygen plasma were performed. Accompanying to the photovoltaic investigations, analytical characterizations of the photo anode material using XRD, SEM and a stereo microscope was investigated. Finally a new process chain combining the best obtained intermediate results enabling highly efficient DSSC could be established.

2. EXPERIMENTAL

2.1 Fabrication of dye sensitized solar cells

The TiO_2 double layer photo anode was deposited on FTO glass (Solaronix SA, Aubonne, Switzerland) with the dimensions of 15 x 20 mm². The FTO glass was cleaned by acetone and distilled

water (~18 MΩ) in ultrasonic bath each for 15 min. For the first TiO_2 layer a 1 mM suspension of AEROXIDE P25 powder (Evonik Industries AG, Essen, Germany) in isopropanol was spin coated (SP) with a motor and laboratory dc power supply (Ico-Tech, Southport, England) on the FTO glass. Earlier investigations on P25 (Evonik) delivered a typical particle size distribution (vendor information: primary particle size: 13 nm; measured values: d_{10}: 93 nm; d_{50}: 120 nm; d_{90}: 450 nm) showing a highly agglomerated titania [24]. The second layer was deposited by KMPP using an oxidation reaction of a precursor molecule. Details and principles of this method can be found in literature [23]. $TiCl_4$ (>99.0%, Sigma Aldrich, St. Louis, MO, USA) with a feeding rate of 0.5 ml h^{-1} as precursor compound and a reaction gas of 80 % argon and 20 % of oxygen (6.0, Air Liquide, Düsseldorf, Germany) with a gas flow rate of 5 l min^{-1} were used as educts. The power of the 2.45 GHz microwave was set to 800 W and the system pressure to 12 mbar. These special parameters yield in nano sized composite material consisting of TiO_2 nanoparticles. To investigate the influence of the plasma length on the photovoltaic properties, two applicators were used. An applicator of 1 λ length yields a plasma length of ca. 12 cm, and a 5 λ applicator enables a plasma length of ca. 60 cm. The resulting composite particles were *in-situ* deposited as a porous nanoparticle-film onto 500 °C preheated TiO_2 spin coated FTO glass. For the nanoparticle film deposition a mask with the dimensions of 5 x 5 mm² was used defining the size of the photoactive region. To investigate the influence of the layer thickness on the photovoltaic properties, the deposition time in the KMPP process was set to 20 and 40 min. The thickness of each layer was characterized by optical profilometry with 600 µm CWL sensor (FRT MicroProf®, Fries Research & Technology GmbH, Bergisch Gladbach, Germany). For further characterization powder of the KMPP synthesized material was collected by thermophoresis, too. After finishing the KMPP deposition, excessive spin coated TiO_2 layer was removed with a conventional cotton swab down to the previously masked region, which resulted in a double layer photo anode with an area of 25 mm². Subsequently, for the increase of adhesion, reduction of organic residuals and electronically interconnection improvement of particles the anodes were heated (sintered) in an oven at 500 °C for 2 h. Prior to dye adsorption, two double layer TiO_2 photo anodes were post treated by immersing them in a $TiCl_4$ aqueous solution (2 ml $TiCl_4$ in 100 ml distilled water (~18 MΩ)) in a beaker and kept in an oven with 60 °C for 1 h. Additionally, one of this new photo anodes was also treated with an oxygen plasma on a ETCHLAB 200-380 (Sentech, Berlin, Germany), with an oxygen gas flow of 0.1 l min-1 and a power of 30 W.

To investigate the influence of the dye structure on the photovoltaic properties, two types of dyes were used. The first was a ruthenizer 535 (Solaronix SA, Aubonne, Switzerland) which represents the established N719 dye [6] and the second was C101 (Dyesol, Queanbeyan, Australia [25]), possessing an extended π-conjugation system. Both dyes were prepared as a 0.5mM ethanol solution. For sufficient dye adsorption the photo anodes were immersed in the solutions for 4 days at 45 °C. The dye sensitized solar cells were sandwiched by applying a 20 µm thick hot-melt gasket as a spacer (74301, Solaronix SA, Aubonne, Switzerland) between the colored double layer TiO_2 nanoparticle coated FTO glass (anode) and the Pt coated FTO glass (cathode, Solaronix SA, Aubonne, Switzerland). The electrolyte was filled with a vacuum system placing a drop of the electrolyte over a hole in the cathode while evacuating. The hole was afterwards sealed with the hot-melt gasket already used as spacer.

To investigate the influence of the electrolyte on the photovoltaic properties three types of electrolytes were used. The first was an in-house development, ionic liquid based system, further denoted as IL, consisting of the following composition: 5.9362 g propylene carbonate, 0.9060 g 1-methyl-3-propylimidazolium iodide, 0.0471 g iodine, 0.0710 g guanidinium thiocyanate, and 0.4034 g 4-tert-butylpyridine showing a reduced vapor pressure, but a higher viscosity and hence reduced ionic conductivity than acetonitrile based mixtures. The second one was an acetonitrile based electrolyte (called ISE), which was donated by A. Hinsch (Fraunhofer ISE, Freiburg, Germany, in-house development with proprietary composition) and the third was the Iodolyte HI-30 (Solaronix SA, Aubonne, Switzerland), which also contains acetonitrile.

2.2 Characterization

The structure of the P25 powder and also of the both collected powders from the 1 λ and 5 λ plasma zone were investigated by X-ray diffraction (XRD, D8 Advanced, Bruker Corporation, Billerica, USA). The morphology of the photo anodes was characterized by scanning electron microscope (SEM, Zeiss Supra 55, Zeiss, Oberkochen, Germany). The dye adsorption on the surface of the photo anodes was investigated by a stereo microscope with transmission light on a Leica M205C (Leica Camera AG, Wetzlar, Germany) visually. The photovoltaic properties of the DSSCs were studied by photocurrent-photovoltage (I-V)-characterization using a source meter (2600 series, Keithley Instruments, Germering, Germany) under illumination using AM 1.5 solar simulator (LS0308, LOT-Oriel Group Europe, Darmstadt, Germany). The measurement under illumination was performed without a mask, due to a clearly defined anode area of 25 mm². Additionally, electrochemical impedance spectroscopy (EIS) also under illumination was carried out using an Iviumstat (Ivium-Technologies, Eindhoven, Netherlands) at an applied bias of open circuit voltage (VOC) and applied amplitude of 10 mA in the 10^5 to 10^{-2} Hz frequency range.

3. RESULTS AND DISCUSSION

3.1 Process development

With respect to an enhancement of the DSSC efficiency several process parameters have been varied: In addition to previous work [26] a thin layer (5 μm) of nano sized titania (P25) particles have been deposited on the FTO/glass substrate via spin coating (SP). Second two main parameters of the gas phase synthesis (KMPP) were varied, the plasma zone length equivalent to the length of the reaction zone and the deposition time. Especially the latter one has a pronounced impact on the layer thickness. In addition the influence of a titania layer post treatment applying $TiCl_4$ and/or an oxygen plasma was investigated. On the part of the organic compounds two different sensitizers and three different electrolytes with varying composition were tested. All investigated titania photo anodes prepared in this work, applying the above listed individual process parameters and cell fabrication steps, are specified in Table 1.

Table 1. Process conditions of all investigated photo anodes

| Cell	Plasma zone	Thickness spin coated layer (SP) (µm)	Deposition time (KMPP) (min)	Thickness KMPP layer (µm)	Dye	Electrolyte	Post treatment in TiCl$_4$ solution / O$_2$ plasma
1	-	5	-	-	N719	IL	no / no
2	5 λ	-	20	1	N719	IL	no / no
3	5 λ	5	20	1	N719	IL	no / no
4	1 λ	5	20	1	N719	IL	no / no
5	5 λ	5	20	1	N719	HI-30	no / no
6	5 λ	5	20	1	N719	ISE	no / no
7	5 λ	5	20	1	C101	ISE	no / no
8	5 λ	5	20	1	C101	HI-30	no / no
9	5 λ	5	40	3	N719	ISE	no / no
10	5 λ	5	40	3	N719	HI-30	no / no
11	5 λ	5	40	3	N719	HI-30	yes / no
12	5 λ	5	40	3	N719	HI-30	yes / yes

3.2 Influence of the processing conditions on the I-V characteristics

Figure 1 compares the I-V characteristics obtained from DSSCs made of four different TiO$_2$ photo anodes, with the same dye (N719) and electrolyte (IL). The first cell (cell 1) represents only a spin coated TiO$_2$ monolayer, the second (cell 2) a titania monolayer only made from KMPP with the 5 λ plasma zone (deposition time: 20 min), and the third (cell 3) the formation of a double layer by combining both methods. In case of cell 4 the length of the plasma zone was reduced in comparison to cell 3. The ionic liquid (IL) based mixture was taken as electrolyte. The first three cells can be treated as reference cells for the double layer approach. All further changes in the process should be compared with cell 3 considering both photo anode deposition methods. The measured I-V characteristics of the spin coated anode (cell 1) and KMPP anode (cell 2) show almost the same behavior. The combination of both deposition methods (cell 3) delivers a significant property change: On the one hand the open circuit voltage (V_{oc}) with 783 mV is smaller comparing to the previous ones, but the short circuit current (I_{sc}) with 8.01 mA cm^{-2} shows almost a tripling, resulting in an photoenergy conversion efficiency (η) of 3.3 % comparing to 1.7 % (cell 1) and 1.9 % (cell 2). XRD revealed particle sizes of about 25 nm for the spin coating TiO$_2$ layer (P25) and about 1-5 nm for the KMPP layer. The combination of both, SP and KMPP, particle layers enables an improved photovoltaic performance due to the formation of a bimodal system increasing significantly the accessible titania surface area. The smaller particles improve the electron transfer at the photo anode, where they lodge themselves between the large particles and so all particles of the photo anode are connected electronically to each other [6]. The larger particles deliver an increased scattering of the incoming light inside the photo anode and enhance the light harvesting [13]. The scattering of light increases the path length of the photons inside the cell and, thus, increases its probability to interact with a dye molecule and inject an electron into the semiconductor [27]. The formation of the double layer decreases the porosity on the

electrode ground acting as a block layer and reduces the charge recombination between the electrolyte and the FTO glass [28]. This interpretation is schematically illustrated in (Fig. 2) together with microscopic images of the different photo anode surfaces. Additionally, the dye adsorption is also favored by the combination of layers.
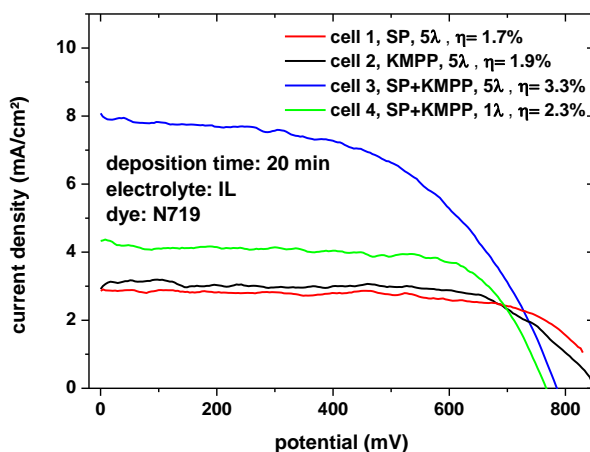
Figure 1. I-V characteristics of cells 1-4 applying different initial process conditions
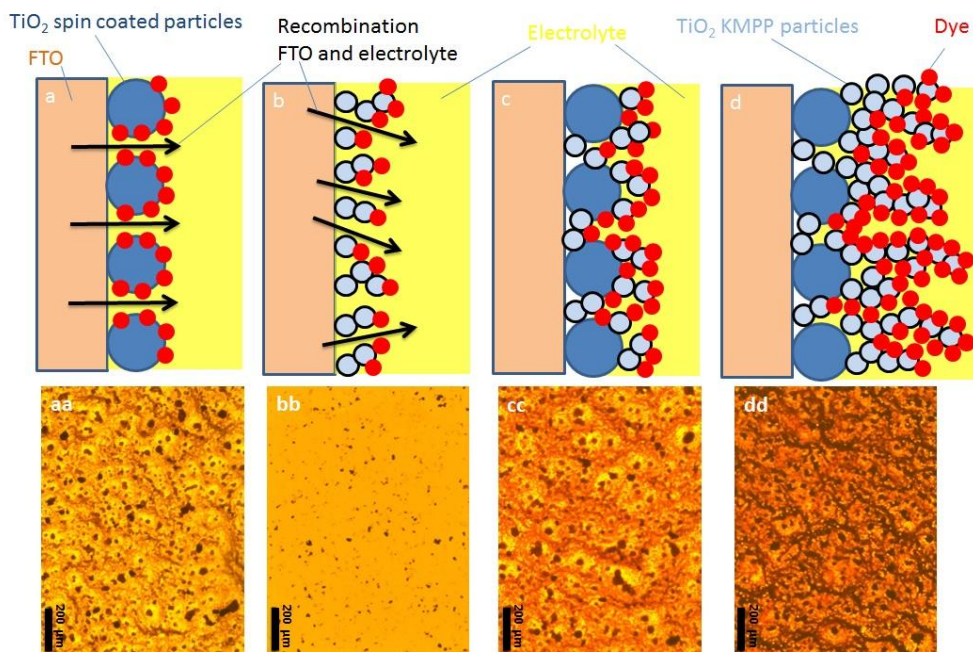
Figure 2. Photo anodes after dye immersing **a)** schematically only spin coated layer (cell 1), **aa)** stereo microscope only spin coated layer, **b)** schematically only KMPP layer (cell 2), **bb)** stereo microscope only KMPP layer, **c)** schematically double layer deposited for 20 min (cell 3), **cc)** stereo microscope double layer deposited for 20 min, **d)** schematically double layer deposited for 40 min, **dd)** stereo microscope double layer deposited for 40 min. The red color in the stereo microscope pictures indicate the optical quantity of dye adsorption on the surface of the photo anodes

**Table 2.** Performance characteristics of cells 1-4

Cell	V_{oc} (mV)	I_{sc} (mA cm^{-2})	FF (%)	η (%)
1	829	2.87	22.1	1.7
2	865	3.10	68.1	1.9
3	783	8.07	52.1	3.3
4	767	4.32	67.9	2.3

This can be seen by comparing the weakly red colored spin coated (Fig. 2, aa) and KMPP (Fig. 2, bb) layers with the homogenously red colored double layer area (Fig. 2, cc). A further increase in the deposition time generates an enlarged titania interfacial surface area and a resulting pronounced dye adsorption (Fig. 2, dd). Consequently, more dye molecules are adsorbed over the whole surface area of the double layer photo anode, which results in an increased photovoltaic performance.

To investigate the influence of the plasma length on the photovoltaic performance cell 3 made with the 5 λ plasma zone was compared with cell 4 made with the 1 λ plasma zone. In both cases a double layer photo anode with the deposition time of 20 min for the second layer, the dye N719 and the electrolyte IL was used. The resulting V_{oc} is almost identical (767 mV), but the I_{sc} is approximately halved (4.32 mA/cm²). Table 2 summarizes the measured cell characteristics of cells 1-4.

3.3 Phase analysis of the deposited titania nanoparticles

The structure of both collected KMPP powders used in cells 3 and 4 was investigated by XRD (Fig. 3). The material used in cell 3 is mainly anatase whereas the diffraction pattern of the electrode synthesized in the 5 λ plasma zone shows a clearly pronounced shoulder at the position of the rutile (110) lattice plane. The exact amount of rutile and anatase phases could not be given quantitatively. As discussed by Song et al. [11], anatase particles possess better inherent photoelectrochemical properties than rutile, while rutile particles exhibit a higher electron transfer. The same author group [11] reported also that the combination of anatase-rutile structure yield in improved I-V characteristics compared to each single structure. Hurum et al. [9] explained the greater photo effectiveness of the combined TiO$_2$ phases due to three factors: (1) the smaller band gap of rutile extends the useful range of photoactivity into the visible region; (2) the stabilization of charge separation by electron transfer from rutile to anatase slows recombination; (3) the atypical small size of the rutile crystallites facilitates this transfer, making catalytic hot spots at the rutile-anatase interface. The improvement of the photovoltaic performance of the photo electrode synthesized in the 5 λ plasma zone is ascribed to the difference in rutile phase compared to the electrode synthesized in the 1 λ plasma zone. The used P25 from Evonik for spincoating is also a mixture of anatase (85 wt%) and rutile (15 wt%) (data supplied by the vendor [29]. This ratio may vary from batch to batch [30].
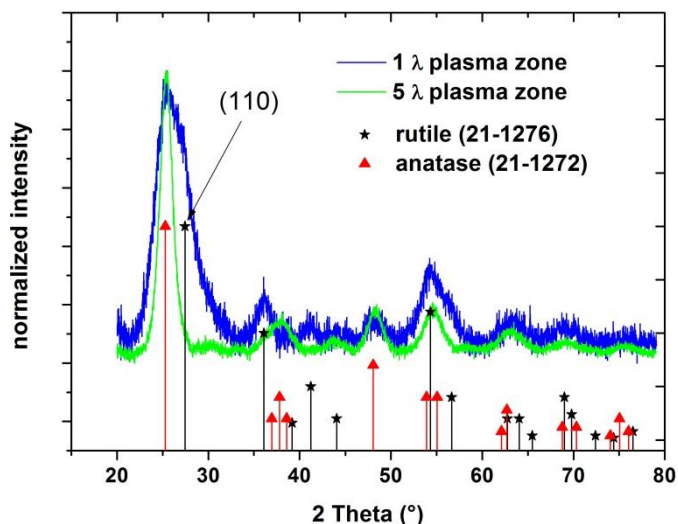
Figure 3. XRD pattern of the powders synthesized in a 1 λ and 5 λ plasma zone

3.4 Influence of the used dye and electrolyte on the I-V characteristics

Considering only the photo anode the best photoelectrochemical performance could be achieved with the double layer, in which the second layer was synthesized with a 5 λ plasma zone, here in combination with the commercial dye N719 and the in-house developed electrolyte IL. To investigate the influence of dye and electrolyte on the photovoltaic properties, the dye C101 and the electrolytes ISE and HI-30 were selected, respectively. Figure 4 and Table 3 show the obtained I-V characteristics of five double layer cells, which are synthesized with the 5 λ plasma zone using a deposition time of 20 min. Cell 5 was combined with the electrolyte HI-30 and dye N719, cell 6 with the electrolyte ISE and dye N719, cell 7 with the electrolyte ISE and dye C101, and, finally, cell 8 with the electrolyte HI-30 and dye C101 (Tab. 1). The obtained I-V characteristics of the cells 3, 5 and 6, applying dye N719 in combination with different electrolytes, show nonuniform photovoltaic results. While cell 3 with the electrolyte IL shows a value for η of 3.3 %, cell 5 with the electrolyte HI-30 delivers an improved efficiency η of 4.6 %. The best performance was obtained with cell 6 and the electrolyte ISE with η=5.1 %. With the applied measurement parameters, the acetonitrile, which is used in HI-30 and ISE, could improve the performance of the photo anode. It is known from electrolyte development for lithium ion batteries that the viscosity of ionic liquid based and organic solvent free electrolytes is significantly higher (up to a factor of 100) than solvent based ones [31-35]. Following the empirical and in electrolyte research widely used Walden rule the ionic conductivity is reciprocal to the viscosity [31-33,36]. This explains the better performance of the acetonitrile based electrolytes (HI-30, ISE) in contrast to the IL based one enabling a better movement of the redox shuttle I^-/I_3^- ions. This is advantageous since the charge transfer is not hindered by poor diffusion. Due to the high vapor pressure of acetonitrile and the resulting loss of solvent, the acetonitrile based electrolyte cannot be used in opposite to the IL at temperatures exceeding 65 °C, which are realistic under full sunlight illumination for several hours. Hence electrolytes for DSSC with reduced vapor pressure are under development [35]. The cells 7 and 8 were immersed in the dye C101 and show in

contrast to the electrodes assembled with dye N719 an inverted efficiency behavior for the both electrolytes (HI-30 and ISE) with a best efficiency of η=5.1 % with the combination C101 and HI-30. It can be concluded, that the photovoltaic performance cannot be interpreted individually depending only on the used dye or electrolyte, but must be seen as a whole system of dye and electrolyte together, especially considering the interfacial behavior between photo anode, dye and electrolyte. Here the cells containing the dye C101 show an increased I_{sc}, a decreased V_{oc} and a reduced filling factor (FF), hence the overall efficiency cannot be improved distinctively. Following these results and considering the higher price for C101 (1g ~ 800 €, Dyesol Ltd.), all further investigations were carried out only with the dye N719 (1g ~ 130 €, Dyesol Ltd.).
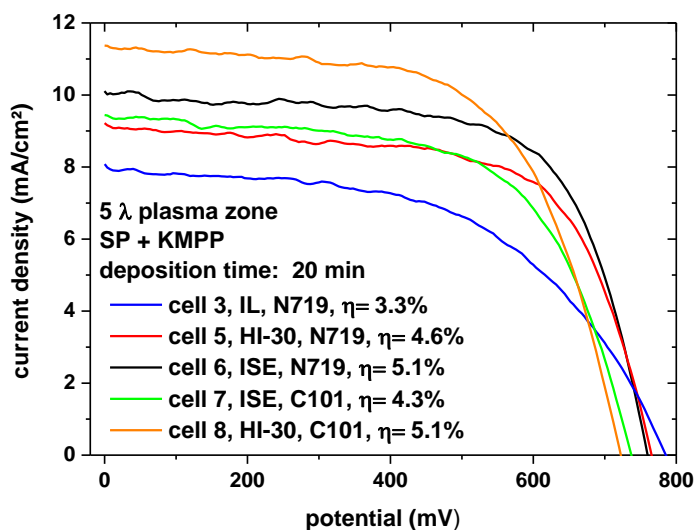

Figure 4. I-V characteristics of cells 5-8; for better comparison cell 3 is also given
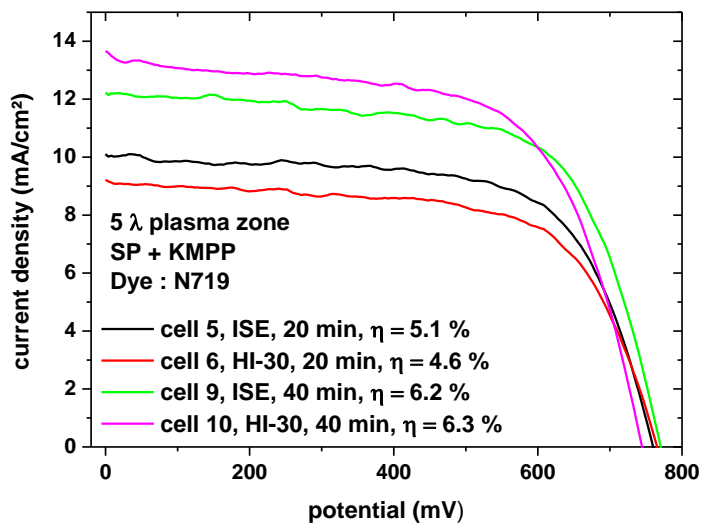
Table 3. Performance characteristics of cells 5-8

Cell	V_{oc} (mV)	I_{sc} (mA cm^{-2})	FF (%)	η (%)
5	763	9.21	65.4	4.6
6	760	10.10	66.1	5.1
7	736	9.39	61.7	4.3
8	722	11.34	62.3	5.1

3.5 Influence of the applied deposition time

In addition to cells with 20 min deposition time (cells 5 and 6) during the KMPP layer deposition step photo anodes with a deposition time of 40 min (cells 9 and 10) were synthesized to investigate the influence of the deposition time on the photovoltaic performance. Afterwards the photo electrodes were immersed in dye N719 and assembled using the electrolytes ISE (cell 9) and HI-30 (cell 10). The resulting I-V characteristics of these cells (Fig. 5, Tab. 4) show for both photo anode-electrolyte combinations an improved photovoltaic performance with a best efficiency value of 6.3% (cell 10). The improved photovoltaic performance for the electrode with extended KMPP layer

deposition time can be attributed to the morphology of the photo anode. The difference in layer morphology of the anodes is shown in (Fig. 6). Compared to the photo anode deposited for 20 min (Fig. 6a) the photo anode deposited for 40 min (Fig. 6b) shows a coarser morphology with a more porous surface structure.

Figure 5. I-V characteristics of cell 9 and 10; the curves of cell 5 and 6 are given again to ease comparison

Table 4. Performance characteristics of cells 9-12

| Cell	V_{oc} (mV)	I_{sc} (mA cm^{-2})	FF (%)	η (%)
9	770	12.19	66.2	6.2
10	744	13.70	63.1	6.3
11	756	23.54	51,3	9.1
12	782	21.35	51.9	8.7
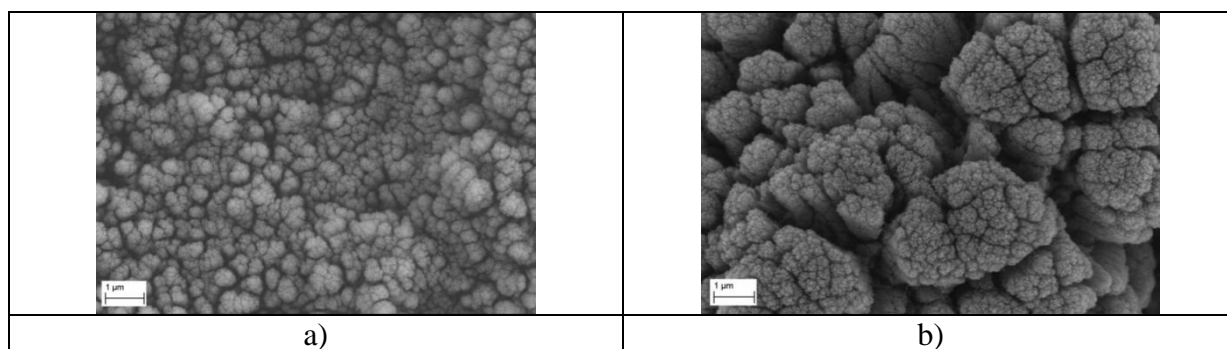
Figure 6. SEM pictures of the photo anodes with a KMPP deposition time of a) 20 min and b) 40 min. It can be noted, that the longer deposition time creates a coarser morphology with a more porous surface structure.

This seems to favor the adsorption of dye and wettability with electrolyte due to the increased accessible surface area. The improved dye adsorption is visible in (Fig. 2) by comparing the photo anode with 20 min KMPP deposition time (Fig. 2, cc) with the photo anode synthesized using 40 min (Fig. 2, dd). The anode deposited for 40 min clearly indicates a more red colored surface area compared to the anode deposited for 20 min. Due to this increased dye adsorption an improved photovoltaic performance can be explained.

3.6 Influence of post treatment

As an additional process step the titania nanoparticles can be post treated after deposition applying an $TiCl_4$ solution solely or in combination with an oxygen plasma prior to $TiCl_4$ immersion for a further surface modification. Figure 7 and Table 4 compare the I-V characteristics of three different cells with a double layer photo anode, synthesized with a 5 λ plasma zone for 40 min, using N719 and electrolyte HI-30. The photo anode of cell 10 was taken as described earlier without post treatment, the anode of cell 11 was post treated in the $TiCl_4$ solution and finally the photo anode of cell 12 was post treated in the $TiCl_4$ in combination with the oxygen plasma.

The I-V characteristics demonstrate a further improvement of photovoltaic performances for the post treated cells. Whereas the I_{sc} of the post treated cells is increased significantly the V_{oc} is nearly unchanged. With an I_{sc} of 23.54 mA cm^{-2}, the short circuit current of cell 11 (post treated with $TiCl_4$) is almost doubled in comparison to cell 10 (without any post treatment) showing an I_{sc} of 13.70 mA cm^{-2}. It is known, that structural defects and cracks may occur during the process of high temperature sintering of TiO_2 nanoparticle films [15,37,38].
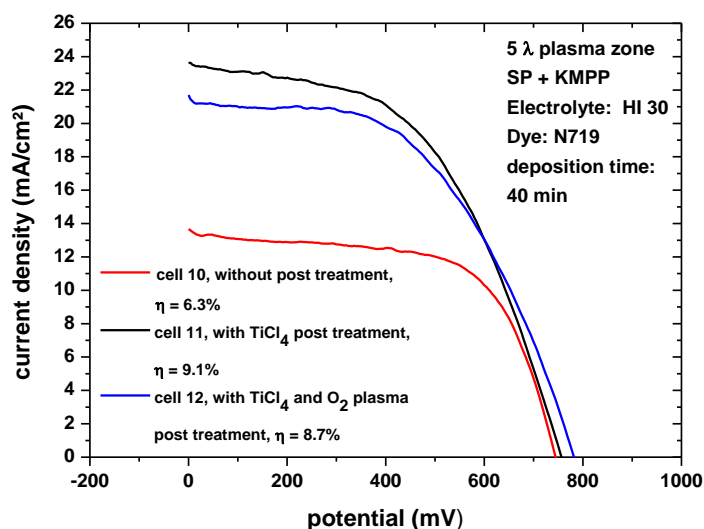
Figure 7. I-V characteristics of cell 11 and 12; cell 10 is given again for comparison

Accordingly, the defects and cracks may induce a higher chance of charge recombination by trapping electrons at the surface of defects and cracks. With $TiCl_4$ post treatment a thin blocking layer

of TiO_2 was deposited on the TiO_2 surface and thus improved the surface morphology. Consequently, charge recombination could be reduced and charge transport could be enhanced [15-17]. The difference of morphologies between the photo anodes, with and without a $TiCl_4$ post treatment, was characterized by SEM and can be seen in Figure 8. Compared to the photo anode without post treatment (Fig. 8a) with a cauliflower-like structure the photo anode with post treatment (Fig. 8b) shows a more glazed surface structure. This indicates an additional, thin covering layer on top of the post treated photo anode, which is assumed to be a TiO_2 blocking layer resulting from $TiCl_4$ solution.
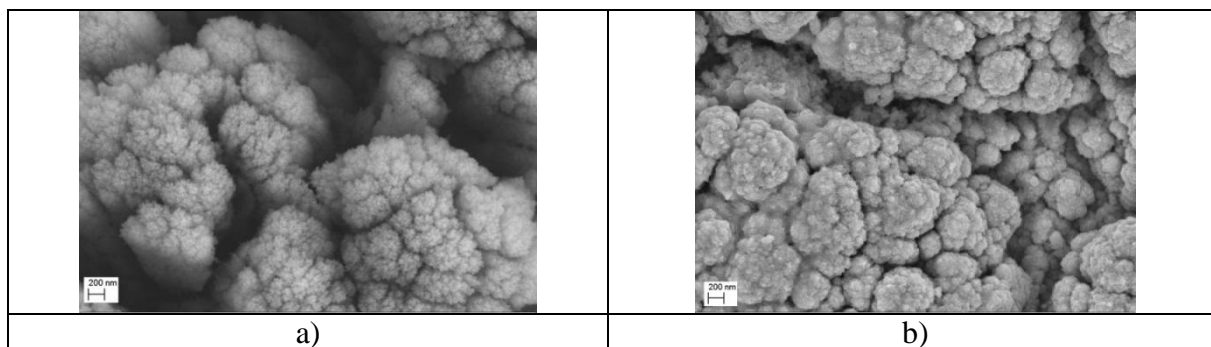

Figure 8. SEM pictures of the photo anodes a) without and b) with a $TiCl_4$ post treatment. The photo anode without post treatment shows a cauliflower-like morphology resulting from particle film deposition in the KMPP process whereas the post treated photo anode shows a glazed surface structure. This indicates an additional, thin covering layer of the post treated photo anode, which is assumed to be a TiO_2 blocking layer resulting from $TiCl_4$ solution.

The advantage of a subsequent oxygen plasma treatment was described by various groups [15,18,19] and ascribed to an increased hydrophilicity promoting the dye attachment on the TiO_2 surface, could not be verified by our experimental results. Moreover, the photovoltaic performance of the oxygen plasma treated photo anode instead indicates a slight deterioration of efficiency from $\eta = 9.1\%$ for the non-plasma treated photo anode to $\eta = 8.7\%$ for the plasma post treated one. The obtained efficiency values are in good agreement with current research data published in literature using different approaches for the synthesis of titania based photo anodes (double layer: P25 with Ag decorated titania: 9% [21]; titania nanotubes: 8.1% [22]; double layer: P18 with dice-like anatase: 8.7% [39]). The use of a double layer approach seems therefore to be advantageous.

3.7 Cell impedance measurement

Electrochemical impedance spectroscopy (EIS) is a powerful technique to characterize electronic or ionic transport process in DSSCs, typically used for the measurement of the internal resistance of electrochemical cells. Figure 9 shows the Nyquist plots of the investigated cells 7-12. The semicircles in the Nyquist plot correspond to I^-/I_3^--transport in the electrolyte, electron recombination at the TiO_2/electrolyte interface together with electron transport in the TiO_2 network, and charge transfer at the counter electrode in the order of increasing frequency [40]. It can be seen, that the EIS

measurements are consistent with the photovoltaic data. With decreasing semicircle values, indicating impedance (electrical and ionic resistance) decrease, the photovoltaic data improves (Fig. 5 and 7). The smallest impedance values can be obtained in case of cells 11 and 12 corresponding with the highest conversion efficiencies around 9 %.
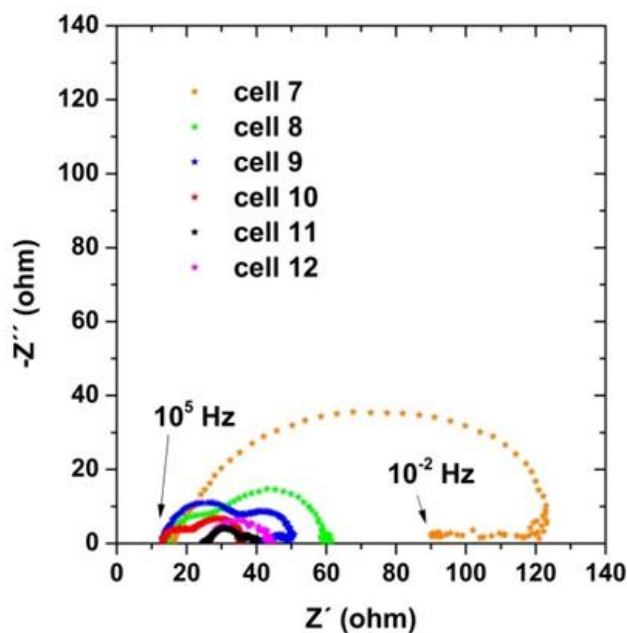
Figure 9. Nyquist plot for six DSSCs

4. CONCLUSION

In this work a new process chain for the realization of a double layer titania based photo anode for the formation of a high performance DSSC was developed. Systematically different parameters and materials influencing the photovoltaic properties have been varied targeting huge conversion efficiency. Initially, a double layer structure, consisting of a spin coated TiO_2 (commercial P25) layer and a TiO_2 layer synthesized in the 5 λ plasma zone of the Karlsruhe Microwave Plasma Process (KMPP), is found to be beneficial for the photovoltaic properties. This is explained with the advantageous association of smaller and larger particles forming a compact block layer and therefore reducing charge recombination with the FTO substrate. In addition, the longer deposition time for the KMPP layer is found to create a coarser morphology with a more porous surface structure, which obviously favours dye adsorption and wettability with electrolyte. Furthermore, the influence of dye and electrolyte on the photovoltaic performance cannot be interpreted individually and separated by each other since dye and electrolyte are building a closely related charge carrier system. The best performance was obtained when using a photo anode post treatment in a $TiCl_4$ solution, creating a thin covering and blocking layer of TiO_2, resulting in an I_{sc} of 23.54 mA cm^{-2}, V_{oc} of 756 mV and a good efficiency η of 9.1 %.

References

1. R.W. Miles, G. Zoppi, and I. Forbes, *Materials Today*, 10(11) (2007) 20-27.
2. A. Luque and S Hegedus (Eds.), Handbook of Photovoltaic Science and Engineering, J. Wiley & Sons, Chichester, England, 2003.
3. P. Wuerfel, Physics of Solar Cells, 2nd updatzed and expanded edition, Wiley-VCH, Weinhein, Germany, 2009.
4. B. O'Regan and M. Graetzel, *Nature*, 353(6346) (1991) 737-740.
5. M. Graetzel, *Journal of Photochemistry and Photobiology C: Photochemistry Reviews*, 4 (2003) 145-153.
6. M Graetzel, Inorganic Chemistry, 44 (2005) 6841-6851.
7. www.nrel.gov/ncpv/images/efficiency_chart.jpg; access 08.06.2015
8. F. Gao, Y. Wang, D. Shi, J. Zhang, M. Wang, X. Jing, R. Humphry-Baker, P. Wang, S.M. Zakeeruddin and M. Grätzel, *Journal of the American Chemical Society*, 130(32) (2008) 10720-10728
9. D.C. Hurum, A.G. Agrios, K.A. Gray, T. Rajh and M.C. Thurnauer, *The Journal of Physical Chemistry B*, 107(19) (2003) 4545-4549
10. W. Li, C. Liu, Y. Zhou, Y. Bai, X. Feng, Z. Yang, L. Lu, X. Lu and K.-Y. Chan, *The Journal of Physical Chemistry C*, 112(51) (2008) 20539-20545
11. X.-M. Song, J.-M. Wu, M.-Z. Tang, B. Qi and M. Yan, *The Journal of Physical Chemistry C*, 112(49) (2008) 19484-19492
12. H. Wang and J. Bell,. 2007, SPIE Proceedings BioMEMS and Nanotechnology III, SPIE Vol 6799 (2007) 67990E-1 67990-7
13. S. Hore, C. Vetter, R. Kern, H. Smit and A. Hinsch, *Solar Energy Materials and Solar Cells*, 90(9) (2006) 1176-1188
14. A. Usami, *Chemical Physics Letters*, 277(1–3) (1997) 105-108
15. X. Xin, M. Scheiner, M. Ye and Z. Lin, *Langmuir*, 27(23) (2011) 14594-14598
16. B. Liu and E.S. Aydil, *Journal of the American Chemical Society,* 131(11) (2009) 3985-3990
17. G.K. Mor, K. Shankar, M. Paulose, O.K. Varghese and C.A. Grimes, *Nano Letters,* 6(2) (2005) 215-218
18. J. Wang and Z. Lin, *Chemistry of Materials*, 22(2) (2009) 579-584
19. K.-H. Park and M. Dhayal, *Electrochemistry Communications*, 11(1) (2009) 75-79
20. M. Ye, X. Wen, M. Yang, J. Iocozzia, N. Zhang, C. Lin, and Z. Lin, *Materials Today*, 18 (2015) 155-162
21. L. Zhao, C. Zhong, Y. Wang, S. Wang, B. Dong, and L. Wan, Journal of Power Sources, 292 (2015) 49-57
22. T. Zeng, H. Ni, X. Su, Y. Chen, and Y. Jiang, Journal of Power Sources, 283 (2015) 443-451
23. T. Hanemann and D.V. Szabó, *Materials*, 3(6) (2010) 3468-3517
24. T. Hanemann, Polymer Composites, 34(9) (2013) 1425-1432
25. http://www.dyesol.com/products/dsc-materials/dyes/c101-dye.html, access 08.06.2015
26. H. Yang, D.V. Szabó, S. Schlabach, and T. Hanemann, Poster presentation at 2nd International Conference on Materials for Energy (EnMat 2013), 12.-16. May 2013, Karlsruhe, Germany

27. C.J. Barbé, F. Arendse, P. Comte, M. Jirousek, F. Lenzmann, V. Shklover and M. Grätzel, Journal of the American Ceramic Society, 80(12) (1997) 3157-3171

28. P.J. Cameron and L.M. Peter, The Journal of Physical Chemistry B, 107(51) (2003) 14394-14400

29. http://www.aerosil.com/sites/lists/IM/Documents/AEROSIL-technical-overview-DE.pdf, access 09.06.2015

30. M. Mehrvar, W.A. Anderson, and M. Moo-Young, *International Journal of Photoenergy*, 04 (2002) 141-146

31. C. Schreiner, S. Zugmann, R. Hartl and H.J. Gores, *Journal of Chemical & Engineering Data*, 55(5) (2009) 1784-1788

32. C. Schreiner, S. Zugmann, R. Hartl and H.J. Gores, *Journal of Chemical & Engineering Data*, 55(10) (2010) 4372-4377

33. S.-Y. Lee, K. Ueno and C.A. Angell, *The Journal of Physical Chemistry C*, 116(45) (2012) 23915-2

34. A. Hofmann, M. Schulz, S. Indris, R. Heinzmann, and T. Hanemann, *Electrochimica Acta*, 147 (2014) 704-711

35. A. Hofmann, F. Kiliani, and T. Hanemann, Poster presentation at 65th Annual Meeting of the International Society of Electrochemistry, 31.08.-05.09.2014, Lausanne, Switzerland.

36. A. Hofmann, M. Schulz, and T. Hanemann, *International Journal of Electrochemical Science*, 8 (2013) 10170-10189

37. J. Wang and Z. Lin, *Chemistry of Materials*, 20(4) (2008) 1257-1261

38. K. Zhu, T.B. Vinzant, N.R. Neale and A.J. Frank, *Nano Letters*, 7(12) (2007) 3739-3746

39. X. Wei, J. Liu, and X.-W Liu, *Solar Energy Materials & Solar Cells*, 134 (2015) 133-139

40. D. Kuang, C. Klein, Z. Zhang, S. Ito, J.-E. Moser, S.M. Zakeeruddin and M. Grätzel, Small, 3(12) (2007) 2094-2102